Parameter Estimation with Entangled Photons Produced by Parametric Down-Conversion

Hugo Cable[1,*] and Gabriel A. Durkin[2]

[1]*Centre for Quantum Technologies, National University of Singapore, 3 Science Drive 2, Singapore 117543*
[2]*Quantum Laboratory, NASA Ames Research Center, Moffett Field, California 94035, USA*

(Received 19 October 2009; published 1 July 2010; corrected 2 July 2010)

We explore the advantages offered by twin light beams produced in parametric down-conversion for precision measurement. The symmetry of these bipartite quantum states, even under losses, suggests that monitoring correlations between the divergent beams permits a high-precision inference of any symmetry-breaking effect, e.g., fiber birefringence. We show that the quantity of entanglement is not the key feature for such an instrument. In a lossless setting, scaling of precision at the ultimate ''Heisenberg'' limit is possible with photon counting alone. Even as photon losses approach 100% the precision is shot-noise limited, and we identify the crossover point between quantum and classical precision as a function of detected flux. The predicted hypersensitivity is demonstrated with a Bayesian simulation.

DOI: 10.1103/PhysRevLett.105.013603 PACS numbers: 42.50.St, 06.20.Dk

We wish to promote the fitness of two spin-j systems combined in an overall spin zero singlet as a resource for metrology. A photonic implementation of such states is readily and scalably generated using stimulated parametric down-conversion (PDC) [1]. Both their rotational symmetry [2] and persistence of entanglement [3,4] under photonic loss channels has made the singlets natural candidates for quantum key distribution [5]. In this Letter we further highlight their utility, this time in a parameter-estimation protocol. Generally, such protocols are rated by the precision (or uncertainty) associated with unbiased estimation of the unknown parameter, and how quickly this precision is lost under relevant decoherence. We will show that given ideal conditions the singlets allow a precision scaling at the Heisenberg limit (the ultimate limit for linear quantum processes, and for which noise scales as $1/N$ with respect to the light intensity or particle number N). Under incoherent photon loss measurement precision is naturally degraded, but at a much gentler rate than other proposals [6] where the decay can be exponential in N. (Recently, the role of photon losses in optical precision experiments was examined carefully [7].)

Consider an instrument broken down into three components [8]: pure probe state $|\psi\rangle$, unitary evolution $U = \exp(-i\hat{H}t)$ under a time-independent Hermitian Hamiltonian $\hat{H}$, and complete projective measurements, $\hat{M} = \sum_i m_i|i\rangle\langle i|$, where $\langle i|j\rangle = \delta_{ij}$. We wish to infer evolution time t from frequencies of outcomes m_i, but t may equally represent an interferometer phase, a magnetic or gravitational field, or some other real-valued continuous variable. Extrapolating from a set of parameter-dependent measurements to an estimation of that parameter can be a challenging task. The probability distributions for individual outcomes are often non-Gaussian, having multiple peaks or broad tails. Quite separate from designing a good estimator from measurement data, it is as important to employ measurements sensitive to small changes in the unknown parameter. An optimal measurement should also, if possible, achieve highest estimation precision for all parameter values. Conditions for identifying optimal measurements were identified in early work on quantum Fisher information. One parameter-independent approach uses canonical measurements, but these are hard to implement directly [9]. In other proposals, measurements are optimal near particular ''sweet spots'' in parameter space, and require multistep adaptive measurements to exploit them [10].

We first present a protocol in a decoherence-free setting for which our proposed measurements are optimal, parameter-free and practicable; they may be realized in a laboratory by photon-counting or spin projections. We extend the analysis to consider realistic decoherence. Translating our protocols to a quantum-optics setting, characterized by a PDC source, we evaluate the effect of photon losses (in transmission and detection) on precision. It emerges that spin-projection measurements are no longer optimal or parameter independent. Nonetheless, precision is always at least as good as the classical upper bound (noise scaling $\propto N^{-1/2}$, called the shot-noise limit) for *any* loss.

Input states.—Let us introduce the states in the spin representation [11]. Our probe is a bipartite maximally entangled spin singlet

$$|\psi_0^{(j)}\rangle = \frac{1}{\sqrt{2j+1}} \sum_{m=-j}^{+j} (-1)^{j-m} |j, m\rangle_{za} \otimes |j, -m\rangle_{zb} \quad (1)$$

labeling component spaces a and b. This state has total spin $J = 0$: $\langle\psi_0^{(j)}|\vec{J}^2|\psi_0^{(j)}\rangle = 0$ where $\vec{J} = (\vec{J}_a + \vec{J}_b)$. The singlet is ''rotationally'' invariant [2] under $U_a^{(j)}(g_1) \otimes U_b^{(j)}(g_2)$ when $g_1 = g_2 \in \mathrm{SU}(2)$; its description in Eq. (1) is identical in any spin basis, e.g. $z \mapsto x \mapsto y$, and the state's properties change only with the *relative* transformation $\mathbb{1}_a \otimes U_b^{\dagger(j)}(g_1) U_b^{(j)}(g_2)$. There is an application here for relative measurements made between nonlocal observers; global phenomena are excluded.

Phase-estimation protocol.—Examine now the estimation of a relative phase ϕ accumulating between a and b. Breaking the symmetry of $|\psi_0^{(j)}\rangle$ by applying $\mathbb{1} \otimes U_b^{(j)}$, yields the state $|\psi_\phi^{(j)}\rangle = \exp(-i\phi \hat{J}_{yb})|\psi_0^{(j)}\rangle$ if we choose rotation about y. In the paradigm above, $\hat{H} \mapsto \hat{J}_{yb}$ and $t \mapsto \phi$. Then make projective measurements onto the basis of z eigenstates for a and b, i.e., $\hat{M} \mapsto \hat{J}_{za} \otimes \hat{J}_{zb}$. The probabilities for the $(2j+1)^2$ measurement outcomes (A, B) are

$$P_{AB}(\phi) = |\langle j, A|_{z,a}\langle j, B|_{z,b}|\psi_\phi\rangle|^2 = \frac{d^{(j)}_{B,-A}(\phi)^2}{(2j+1)}. \quad (2)$$

Note that $P_{AB}(\phi) = P_{AB}(-\phi)$, and to eliminate ambiguity the range of ϕ can be restricted to $[0, \pi]$.

Quantifying precision.—To establish this scheme's performance we employ classical Fisher information $I_{\rm cl}(\phi) = \sum_{A,B} P_{A,B}[\frac{d}{d\phi}\ln(P_{A,B})]^2$. It provides a distance metric in probability space, e.g for $\epsilon \ll 1$ the distance between $P_{AB}(\phi)$ and $P_{AB}(\phi+\epsilon)$ is $\epsilon\sqrt{I_{\rm cl}}$. A lower bound on the variance of any unbiased estimator of ϕ is $I_{\rm cl}^{-1}$ [12]. Given an unknown rotation by ϕ about the yb axis a short calculation [13] using Eq. (2) gives $I_{\rm cl}(\phi) = 4j(j+1)/3$, independent of ϕ and achieving the quadratic scaling characteristic of the Heisenberg limit (identifying a spin-j state as a composite of $2j$ spin one-half particles, the singlet then has particle number $N = 4j$ and $I_{\rm cl} \propto N^2$).

The quantum Fisher information $I_{\rm qu}$, provides a saturable upper bound, $I_{\rm qu} \geq I_{\rm cl}$. It is a function only of probe and dynamics, assuming the best possible measurement without defining it explicitly. For pure probe states, $I_{\rm qu}/4 = \Delta^2\hat{H} = \langle\hat{H}^2\rangle - \langle\hat{H}\rangle^2$ [14]. Using again $\hat{H} \mapsto \hat{J}_{yb}$, $I_{\rm qu} = 4\langle\hat{J}^2_{yb}\rangle = 4\langle\vec{J}^2_b\rangle/3 = 4j(j+1)/3$ by symmetry. Remarkably $I_{\rm qu} = I_{\rm cl}$, and our original measurement choice is optimal and independent of the value of the unknown parameter ϕ, a preferred property of any parameter-estimation scheme [8,15]. We make at this point some observations about entanglement. First, making a comparison between the probe $|\psi_0^{(j)}\rangle$ and Bell states $|\psi_0^{(1/2)}\rangle$ numbering $2j$ (so total particle number $4j$ is the same), we see that the former has much less entanglement than the latter, $\log_2(2j+1)$ e-bits versus $2j$ e-bits, but a greater value for $I_{\rm qu}$, $4j(j+1)/3$ versus $2j$. Second, although the Hamiltonian only operates on the b modes, no phase information is imprinted locally as the reduced state $\rho^{(b)}$ is always maximally mixed—nothing is learned by measurements exclusive to the space in which dynamics occur. One might believe that the dependence of precision on bipartite measurements is due to entanglement. However, we will show it is retained under a disentangling decoherence channel—exhibiting nonlocality without entanglement.

Simulation.—The quantum bound $(\delta\phi)^2 \geq I_{\rm qu}^{-1}$ on mean-squared error is attainable given infinite repetitions of the experiment (using maximum-likelihood estimation), but superior convergence of the high-j singlets may also be shown when the number of samplings is relatively small, the *preasymptotic* regime. A Bayesian protocol, considered in Fig. 1, compares performance of higher-j singlets with Bell singlets, so that the same total energy is detected in both cases. We use data sequences with k updates of the (uniform) prior distribution $P_0 = 1/\pi$ given measurements $\{A_i, B_i\} = \{A_1, B_1, A_2, B_2, \ldots, A_k, B_k\}$. Each sequence leads to a single ϕ estimate that is the mean of the final posterior distribution P_k. The conditional probability $P(\{A_i, B_i\}|\phi)$ is determined from Eq. (2). The update rule is $P_k(\phi|\{A_i, B_i\}) \propto P(\{A_i, B_i\}|\phi)P_0(\phi)$ and measurement events are independent, so $P(A_1, B_1, A_2, B_2|\phi) = P(A_1, B_1|\phi)P(A_2, B_2|\phi)$. In our simulation, we perform a total of ν independent phase estimates for each choice of parameters j and k, and the total particle resource is $4\nu jk$. We find that the experimental error bars approach the theoretical limit $\delta\phi = 1/\sqrt{kI_{\rm qu}}$ as the particle number increases; red horizontal error bars (spin-j singlets) are seen to be narrower than corresponding blue ones (Bell states) indicating superior precision of the higher-spin singlets in the preasymptotic regime.

Linear optics and parametric down-conversion.—Now we translate our previous arguments into an optical context using an isomorphism between spins and a pair of harmonic oscillators (Schwinger representation). A PDC process produces entangled photons by interaction of a pump laser field with a nonlinear birefringent crystal. The output is shared among four optic modes, labeled $\{a_h, a_v, b_h, b_v\}$ for spatial directions a, b and horizontal and vertical polarizations h, v. (We use the same notation to denote the associated bosonic annihilation operators.) The down-conversion Hamiltonian is $\hat{H} = \kappa(a_h^\dagger b_v^\dagger - a_v^\dagger b_h^\dagger) + \text{H.c.}$ with κ a coupling strength for the nonlinear process, producing light via application to the vacuum: $\exp(-i\hat{H}t)|0\rangle$. The effective parametric gain is $\tau = \kappa t$. Applying the Schwinger representation to spatial mode

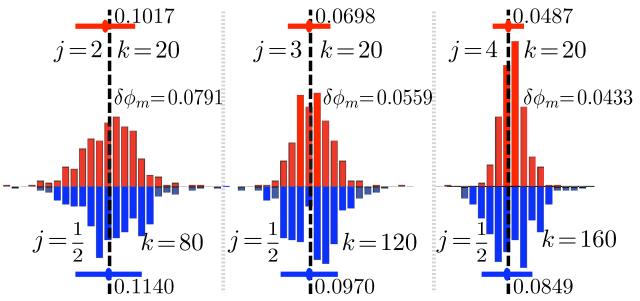

FIG. 1 (color online). Simulation with performance of spin-j singlets (red, above) juxtaposed with spin-1/2 Bell pairs (blue, below), the latter scaling at the shot-noise limit. There were $\nu = 250$ independent phase estimates contributing data points to each of the six charts. A single estimate is obtained after a sequence of $k = 20$ Bayesian updates for probes with $j = 2$, 3, 4 using the distribution of Eq. (2). The true value of ϕ is indicated by black dashed lines. Maintaining the same particle number resource for the Bell probes as the higher-j singlets equates with keeping jk constant. Error bar widths are given to four decimal places.

a: $\hat{J}_{+a} = \hat{a}_h^\dagger \hat{a}_v$, $\hat{J}_{-a} = \hat{a}_h \hat{a}_v^\dagger$, and $2\hat{J}_z = (a_h^\dagger a_h - a_v^\dagger a_v)$ (the number difference). Also $\vec{J}_a^2 = (\hat{n}_a/2)(\hat{n}_a/2 + 1)$, where $\hat{n}_a = (a_h^\dagger a_h + a_v^\dagger a_v)$. Spin quantum numbers map onto photon numbers as $2j_a = (n_{ha} + n_{va})$ and $2m_a = (n_{ha} - n_{va})$. We can now identify each of the elements of our idealized parameter-estimation protocol with a realistic optical source, as explained in Fig. 2. Measurement data can be grouped by photon counting according to values of $j_{a,b}$, equivalent to postselection onto the space of a particular $|\psi_0^{(j)}\rangle$. Optimal correlation measurements $\hat{J}_{za} \otimes \hat{J}_{zb}$ are reconstructed in each $j_{a,b}$-labeled subspace, also from photon counting because $2\hat{J}_{za} = \hat{n}_{ha} - \hat{n}_{va}$. We acknowledge here that efficient photon counting is generally a nontrivial task [16].

Losses.—A realistic analysis must incorporate relevant decoherence; for optic processes incorporating photon counting the important mechanism is that of photon loss, in transmission and detection [4]. Both loss types are effectively modeled by placing partial transmission ($\eta < 1$) beam splitters in the four optic modes in front of perfect detectors, splitting incoming photons into two output modes: the mode transformation is $\hat{a} \mapsto \sqrt{\eta}\hat{a} + \sqrt{1-\eta}\hat{e}$, where $\hat{e}$ is an annihilation operator for the ancillary loss mode. The photons siphoned out of the transmission mode in this way are then traced over. Referring either to modes a or to modes b, if losses are polarization insensitive ($\eta_h = \eta_v$), the loss channel $\mathcal{L}_\eta^h \otimes \mathcal{L}_\eta^v$ commutes with any $U \in \mathrm{SU}(2)$ on the same spatial path: $\mathcal{L}_\eta^h \otimes \mathcal{L}_\eta^v[U\rho U^\dagger] = U(\mathcal{L}_\eta^h \otimes \mathcal{L}_\eta^v[\rho])U^\dagger$ for any ρ. This has two important consequences. First, the nonunitary decoherence due to loss and the unitary ϕ rotation in mode b may be treated independently with impunity. Second, after losses, each component of the PDC state, in a subspace labeled by (j_a, j_b), retains its symmetry under transformations $U_a^{(j_a)}(g) \otimes U_b^{(j_b)}(g)$. This implies a simple, block-diagonal structure for the mixed lossy state

$$\rho^{(j_a,j_b)} = \sum_{J=|j_a-j_b|}^{j_a+j_b} \mu_J^{(j_a,j_b)} \Omega_J^{(j_a,j_b)}. \tag{3}$$

The $\mu_J^{(j_a,j_b)} \in [0, 1]$ are weighting factors [4] and $\Omega_J^{(j_a,j_b)}$ are density operators proportional to identities in each $(2J + 1)$-dimensional orthogonal subspace labeled by total spin J. As symmetry is preserved under loss, the state of Eq. (3) retains a suitability for *relative* measurements between spatially separated observers a and b. We stress that for imperfect transmission $\eta < 1$ there is nonzero occupancy probability for spaces labeled (j_a, j_b), where $j_a \neq j_b$. See Fig. 3(i). Measurements with $n_a \neq n_b$ need not be discarded, they also contribute to overall precision.

Combining subspaces and ultimate precision.—By postselecting onto specific photon numbers (after losses) and filtering the data sets we can focus on a particular (j_a, j_b) subspace and analyze its contribution to overall precision. Fortunately, both I_{qu} and I_{cl} are additive, so total Fisher Information per measurement is the average of the contributions in each subspace weighted by the probabilities of post-selecting each subspace. For the lossless case with $\hat{N} = \hat{n}_a + \hat{n}_b$ we know $I_{\mathrm{qu}} = 4j(j + 1)/3$ (in a space with $n_{a,b} = 2j$ photons) and the ensemble result is $\langle I_{\mathrm{qu}}\rangle = \langle\hat{N}^2\rangle/12 + \langle\hat{N}\rangle/3$. There are associated gains in precision as $\langle\hat{N}\rangle = 4\eta\sinh^2\tau$ increases with τ in the low loss regime. For more significant loss there is a precision trade-off as larger τ are also associated with greater values of decoherence $\theta = (1 - \eta)\tanh\tau$ within each subspace. This may be viewed as higher–photon-number spaces being seeded initially, then as photons are lost these populations make an incoherent contribution to the those of lower photon spaces, ''feeding'' them from above with mixed state components (bad for precision). We illustrate the effect of decreasing transmission η on both subspace weightings in Fig. 3(i), and precision within a subspace, in Fig. 3(ii) (explicitly the $j_a = j_b = 2$ subspace).

Given a general mixed state $\rho = \sum_p \rho_p |p\rangle\langle p|$ Fisher information for unitary evolution under $\hat{H} \mapsto \hat{J}_{yb}$ is $\langle I_{\mathrm{qu}}\rangle = 2\sum_{q,r} \frac{(\rho_q - \rho_r)^2}{\rho_q + \rho_r} |\langle q|\hat{J}_{yb}|r\rangle|^2$. By observing that the PDC is Gaussian, and that loss channel and interferometer components act as Gaussian operations, this functional can be evaluated directly using phase-space methods [17]. Specifically, we employ the fact that squeezed light subject to incoherent photon loss is formally equivalent to a squeezing operator (with a modified parameter) applied to a thermal state. This allows for the a full identification of the spectrum for the lossy PDC state, and for $\langle I_{\mathrm{qu}}\rangle$ to be evaluated directly by finding nonzero contributions to the sum [13]. We arrive at an expression for the complete

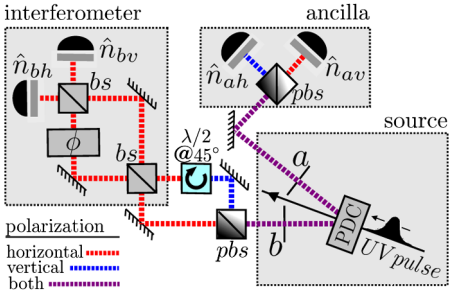

FIG. 2 (color online). Instrument composed of PDC source [1], linear-optical elements (mirrors, phase element ϕ, 50-50 beam-splitters (bs), polarizing beam splitters (pbs), half-wave plate $\lambda/2$), and photocounters. In microscopy or interferometry, modes a may be considered an ancilla or reference; only the photons in modes b interact with the ''sample''. Disregarding losses, the source produces a mixture of spin-j singlets, Eq. (1), with weightings $(2j + 1)\tanh^{4j}\tau/\cosh^4\tau$ determined by the parametric-gain parameter τ. Each singlet has photon-number $N = 4j$, and the overall intensity is $\langle\hat{N}\rangle = 4\sinh^2\tau$ and $\Delta^2\hat{N} = \cosh(4\tau) - 1$. Weightings of higher-photon-number singlets increase with τ but the large $\Delta^2\hat{N}$ indicates a severe flattening of the distribution. We note the immunity of counting measurements to undesired path differences occurring outside of the ''interferometer'' block.

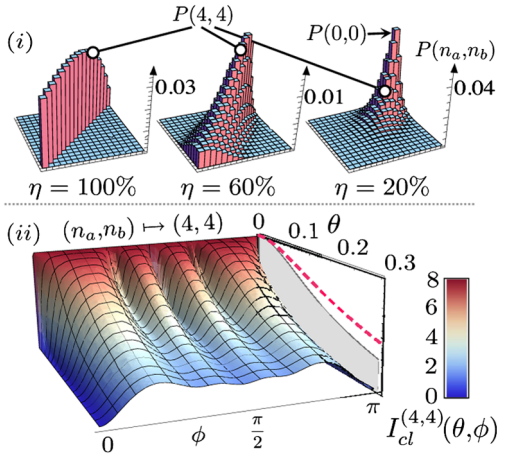

FIG. 3 (color online). (i) Under photon loss the PDC state becomes $\sum P(n_a, n_b)\rho^{(j_a,j_b)}$, where $j_a = n_a/2, j_b = n_b/2$, $\rho^{(j_a,j_b)}$ is given in Eq. (3), and $P(n_a, n_b)$ is a weighting factor for the corresponding subspace [4]. The three plots show $P(n_a, n_b)$ with interaction $\tau \sim 1.83$ and $n_{a,b} \leq 16$. As transmission η is reduced, the weightings of $j_a \neq j_b$ spaces increase and $n_{a,b} \gg 1$ become less probable. In (ii) loss in transmission and detection affects the estimation of ϕ in the $(n_a, n_b) \mapsto (4, 4)$ subspace. The contribution to $\langle I_{\rm cl}\rangle$ is $I_{\rm cl}^{(4,4)}P(4, 4)$. For no losses ($\eta = 1$), $\rho^{(2,2)}$ is the singlet state $|\psi_0^{(2)}\rangle\langle\psi_0^{(2)}|$ and $I_{\rm cl}^{(4,4)} = 8$, contributing to the quadratic precision scaling derived for the lossless case. As losses increase, the precision degrades and $I_{\rm cl}^{(4,4)}$ quickly becomes a function of both ϕ and the decoherence parameter $\theta = (1 - \eta)\tanh\tau$. Blue shading indicates precision below the upper limit for four uncorrelated photons in a classical lossless two-mode interferometer, i.e., $I_{\rm cl} \leq 4$. For $\phi \approx 0.5$ supraclassical precision (red shading) is possible for decoherence $\theta \lesssim 0.2$. This corresponds to loss $\lesssim 26\%$ for $\tau = 1$, an interaction value achieved in real experiments [3]. The maximum $I_{\rm cl}^{(4,4)}$ for each θ value with photon-counting measurements is projected on to the back wall as a grey silhouette—only slightly inferior to $I_{\rm qu}^{(4,4)}$, the best possible for any detection scheme (red dashed line).

Fisher information in terms of transmission η and detection flux $\langle\hat{N}\rangle = 4\eta\sinh^2\tau$:

$$\frac{\langle\hat{N}^2\rangle + 4\langle\hat{N}\rangle}{12} \geq \langle I_{\rm qu}\rangle = \frac{\langle\hat{N}\rangle(4\eta + \langle\hat{N}\rangle)}{8 + 4(1-\eta)\langle\hat{N}\rangle} > \frac{\langle\hat{N}\rangle^2}{8 + 4\langle\hat{N}\rangle}, \quad (4)$$

where the upper and lower limits correspond to $\eta = 1, 0$, respectively. Therefore, even in the worst case, losses approaching 100%, asymptotically $\langle I_{\rm qu}\rangle \sim \langle\hat{N}\rangle/4$ when $\tau \to \infty$ and precision scales $\delta\phi \propto \langle\hat{N}\rangle^{-1/2}$, as with shot noise (in stark contrast to the exponential deterioration in performance of other schemes [6]). As losses increase, flux $\langle\hat{N}\rangle$ can be maintained by turning up the parametric-gain τ, but the Fisher information will inevitably deteriorate because of its separate dependence on η and $\langle\hat{N}\rangle$ above. It is not known whether optimal measurements in the lossy case can be independent of the true parameter value ϕ, certainly photon correlation measurements $\hat{J}_{za} \otimes \hat{J}_{zb}$ are no longer optimal, see Fig. 3(ii). From Eq. (4) it is seen that our scheme performs better than a sample illuminated with coherent light of the same detected flux, for which $\langle I_{\rm qu}\rangle = \langle\hat{N}\rangle/2$, when $\eta > 1/2 + 1/(2 + \langle\hat{N}\rangle)$. Transmission must be better than 50% in the high flux limit to obtain a quantum advantage with PDC.

Summary and outlook.—We have presented a parameter-estimation protocol with several strengths. In a nondissipative environment, Heisenberg scaling is achieved with simple fixed measurements. Our scheme can be implemented using PDC and linear optics, and under severe dissipation (approaching 100%) it is still capable of precision scaling at the shot-noise limit. There exist a variety of applications, such as fiber calibration, the phase microscopy of fragile biological specimens, and optical gyroscopes for GPS-free navigation. The increasing asymmetry of the state with the magnitude of one-sided rotations has a quantifiable utility in reference frame alignment [18].

The authors thank Antia Lamas, Terry Rudolph, and Alessio Serafini for helpful discussions. H. C. acknowledges support for this work by the National Research Foundation and Ministry of Education, Singapore. G. A. D. performed this work under contract with Mission Critical Technologies, Inc.

*cqthvc@nus.edu.sg

[1] A. Lamas-Linares *et al.*, Nature (London) **412**, 887 (2001); M. Rådmark *et al.*, arXiv:0903.2454.
[2] J. Schliemann, Phys. Rev. A **72**, 012307 (2005).
[3] H. S. Eisenberg *et al.*, Phys. Rev. Lett. **93**, 193901 (2004).
[4] G. A. Durkin *et al.*, Phys. Rev. A **70**, 062305 (2004).
[5] G. A. Durkin *et al.*, Phys. Rev. Lett. **88**, 187902 (2002).
[6] X-Y. Chen and L-Z. Jiang, J. Phys. B **40**, 2799 (2007).
[7] M. Kacprowicz *et al.*, Nat. Photon. **4**, 357 (2010).
[8] G. A. Durkin, New J. Phys. **12**, 023010 (2010).
[9] B. C. Sanders and G. J. Milburn, Phys. Rev. Lett. **75**, 2944 (1995); D. W. Berry and H. M. Wiseman, Phys. Rev. Lett. **85**, 5098 (2000).
[10] A. Monras, Phys. Rev. A **73**, 033821 (2006).
[11] Spin notation: $\hat{J}_i|j, m\rangle_i = m|j, m\rangle_i$. Operator $\vec{J}^2 = \sum_{i\in\{x,y,z\}}\hat{J}_i^2$ gives $\vec{J}^2|j, m\rangle_i = j(j+1)|j, m\rangle_i$ and labels subspaces invariant under the action of $SU(2)$. Ladder operators are $\hat{J}_\pm = \hat{J}_x \pm i\hat{J}_y$, and $\hat{J}_\pm|j, m\rangle_z = N_\pm^{(j)}(m)|j, m \pm 1\rangle_z$, where $N_\pm^{(j)}(m) = \sqrt{(j \mp m)(j \pm m + 1)}$. Wigner's rotation matrix is $d_{m',m}^{(j)}(\phi) = \langle jm'|_z \exp(-i\hat{J}_y\phi)|jm\rangle_z$.
[12] G. A. Durkin and J. P. Dowling, Phys. Rev. Lett. **99**, 070801 (2007).
[13] See supplementary material at http://link.aps.org/supplemental/10.1103/PhysRevLett.105.013603.
[14] S. L. Braunstein *et al.*, Ann. Phys. (Leipzig) **247**, 135 (1996); S. Boixo *et al.*, Phys. Rev. Lett. **98**, 090401 (2007).
[15] O. E. Barndorff-Nielsen and R. D. Gill, J. Phys. A **33**, 4481 (2000); H. F. Hofmann, Phys. Rev. A **79**, 033822 (2009).
[16] D. Rosenberg *et al.*, Phys. Rev. A **71**, 061803(R) (2005).
[17] M. Aspachs *et al.*, Phys. Rev. A **79**, 033834 (2009).
[18] G. Gour *et al.*, Phys. Rev. A **80**, 012307 (2009).